Core Electrostatic Fluctuations and Particle Transport in a Reversed-Field Pinch

J. Lei, P. M. Schoch, D. R. Demers, U. Shah, and K. A. Connor
ECSE Department, Rensselaer Polytechnic Institute, Troy, New York 12180

J. K. Anderson
Physics Department, University of Wisconsin, Madison, Wisconsin 53706

T. P. Crowley
National Institute of Standards and Technology, Boulder, Colorado 80305
(Received 5 August 2002; published 17 December 2002)

Potential and electron-density fluctuation profiles, $\tilde{\phi}(r)$ and $\tilde{n}_e(r)/n_e$, are measured for the first time in the core of a reversed-field pinch using a heavy ion beam probe. It is found that the fluctuations are broadband and correlated with the core resonant $m/n = 1/6$ tearing mode. The electrostatic-fluctuation-induced particle transport in the core of standard RFP plasmas, estimated from measured $\langle \tilde{n}_e \tilde{\phi} \rangle$, is small compared to the total particle flux. Measurements of fluctuations and estimates of fluctuation induced particle transport in improved confinement RFP discharges are also presented.

DOI: 10.1103/PhysRevLett.89.275001 PACS numbers: 52.55.–s

The reversed-field pinch (RFP) belongs to the class of magnetic confinement configurations that are driven towards a minimum energy state that can be described by Taylor's theory [1]. Compared to tokamaks and stellarators, RFP plasmas usually have much larger density and potential fluctuation levels which may be largely related to substantial magnetic fluctuations that may be needed to sustain the Taylor state [2]. Large fluctuation levels in turn limit the confinement time of the RFP to milliseconds, which is much smaller than that of a tokamak. In general, people believe that interactions among various fluctuations are the cause of large particle and energy transport that limit the confinement time of magnetic plasma devices [3]. For the Madison Symmetric Torus (MST) RFP, it has been found that the electrostatic fluctuations can account for significant edge particle losses but not energy losses [4]. However, almost no experimental information has been obtained on localized electrostatic fluctuations and their interactions in the core of the RFP. The heavy ion beam probe (HIBP) is well known for its ability to make local measurements of the plasma potential ϕ, potential fluctuations $\tilde{\phi}$, and density fluctuations $\tilde{n}_e/n_e$ in magnetically confined plasmas. The beam does not perturb the plasma which it probes; thus the electrostatic fluctuation induced particle and energy fluxes can be addressed. HIBPs have been successfully applied on tokamaks and stellarators [5–9], but this is the first time a beam probe is used to diagnose the hot core of an RFP. A few factors have made the HIBP measurements challenging: highly three-dimensional, low amplitude magnetic field ($\sim$0.3 T, and $B_\theta \sim B_\phi$) largely determined by the plasma current itself and not well known, small signal levels due to the small electron impact ionization cross section of the Na^+ ions being used, and small diagnostic ports on MST.

The schematic of the MST-HIBP system is shown in Fig. 1. Singly charged or primary ions are injected into the plasma by an accelerator. Typical ion species used by this probe (for the data presented) are Na^+ and K^+ with energies ranging from 40 to 70 keV. The primary beam changes direction in the plasma mainly due to the Lorentz force proportional to $\mathbf{v} \times \mathbf{B}$. Along the primary beam trajectory in the plasma, the beam ions are further ionized to higher charge states (doubly) mainly through electron impact ionizations. The higher charge state ions diverge from the primary ion trajectory due to increased Lorentz forces. Only those secondary ions from a limited ionization location reach the energy analyzer. The plasma potential fluctuation is equal to the energy fluctuation of

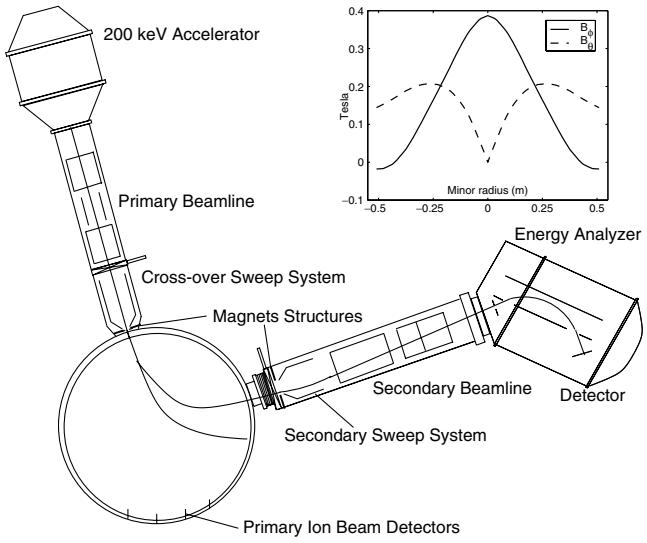

FIG. 1. Schematic of the MST-HIBP system. The inset shows radial variation of the toroidal and poloidal magnetic fields.

the detected secondary ions, while the plasma density fluctuation $\tilde{n}_e/n_e$ is proportional to the fluctuation in intensity of the detected secondary ion current. Because of the fact that the poloidal and the toroidal magnetic fields B_θ and B_ϕ are comparable in MST (see the inset plot of Fig. 1), singly and doubly charged ions travel along fairly complicated three-dimensional paths. In order to get signals out from the MST-HIBP, actual primary and secondary beam lines are toroidally tilted a little bit (not shown in Fig. 1). Also the entrance and the exit ports are separated by 10° in the toroidal direction [10].

Typical MST-HIBP signals of a standard RFP discharge are shown in Fig. 2. The plasma current I_p, line averaged electron-density n_{e0}, reversal factor F $[=B_\phi(a)/\langle B_\phi\rangle]$, core dominant mode speed v, plasma potential ϕ, and secondary intensity signal I_s over a few sawtooth cycles during the flattop period are shown. In the MST plasma, the core dominant mode is $m/n = 1/6$, where m and n are poloidal and toroidal mode numbers, respectively. The power spectra of $\tilde{\phi}$ and $\tilde{n}_e/n_e$ as well as their coherence and phase are plotted in Fig. 3. The HIBP signals are digitized at 1 MHz, thus enabling the resolution of fluctuations from 0 to 500 kHz. Plots are truncated at 100 kHz in the figure due to the observation that above 100 kHz, fluctuation powers become too small to affect the measured total fluctuation levels and electrostatic particle flux. The spectra are calculated from an ensemble of 199 events, with each event having a time period of 0.5 msec, during which the RFP plasma may be treated as being in a quasistationary state.

It has been found that the potential fluctuations peak at the core resonant tearing mode frequencies (Doppler frequency) in the power spectra, yet the low frequency components that correspond to fast equilibrium changes or $m = 0$ modes dominate the total power. However, the density fluctuations, $\tilde{n}_e/n_e$, that are coherent with the core resonant tearing modes' frequencies dominate the power spectrum. This observation is consistent with the fact that the HIBP gives a local measurement of $\tilde{n}_e/n_e$, while localized $\tilde{\phi}$ measurements may be affected by edge electric field fluctuations that have $m = 0$ structures. The small peak in the $\tilde{n}_e/n_e$ power spectra below 10 kHz may be due to a path effect that is caused by density fluctuations along the beam trajectory [11].

The fluctuation profiles $\tilde{\phi}(r)$ and $\tilde{n}_e(r)/n_e$ are obtained by changing the injection angles of the diagnostic beam using the probe's novel crossover sweep system [10]. These profiles are shown in Fig. 4. These measurements are made in the standard plasmas with $I_p \sim 380$ kA, $n_e \sim 10^{13}$ cm^{-3}. The measured $\tilde{\phi} \sim 30$–50 V$_{\rm rms}$, $\tilde{n}_e/n_e \sim 0.1$–0.18 within the measurement range of $r/a = 0.25$–0.75. Error bars indicate standard deviations.

Potential and density fluctuation measurements have also been obtained in improved confinement plasmas. Improved confinement is achieved by current profile modification using an inductive pulsed poloidal current drive (PPCD) technique. PPCD plasmas with parameters similar to those of the standard discharges ($I_p \sim 390$ kA, $n_e \sim 10^{13}$ cm^3) give a measured $\tilde{\phi} \sim 30$ V$_{\rm rms}$ and $\tilde{n}_e/n_e \sim 0.1$ and are relatively flat within the

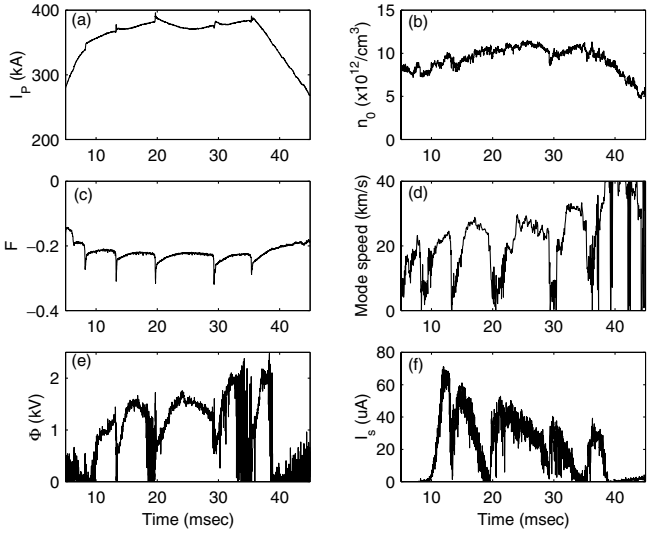

FIG. 2. MST-HIBP signals (Shot No. 1010624039): (a) plasma current; (b) plasma density; (c) reversal factor F; (d) $m/n = 1/6$ mode speed; (e) plasma potential measured by the HIBP; (f) HIBP secondary ion current. Note: The sharp drops in the plasma potential that coincide with dips in F are instrumental in nature and do not necessarily reflect the true plasma potential.

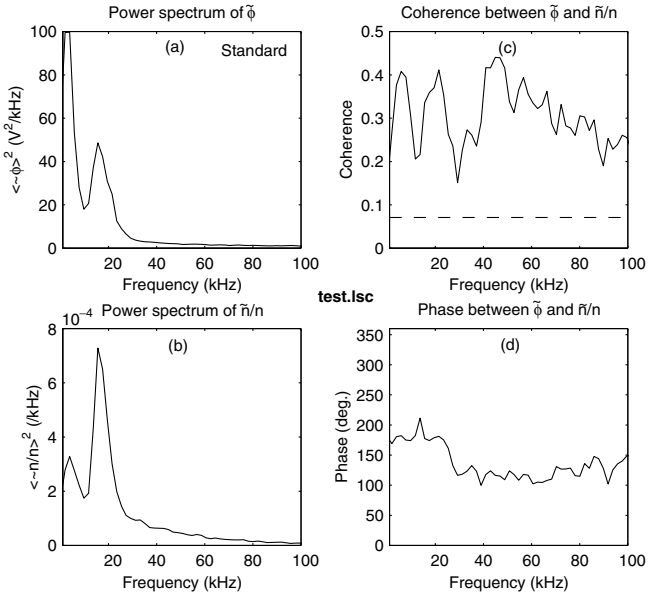

FIG. 3. Power spectra, coherence, and phase of fluctuations for the 380 kA standard plasmas: (a) power spectrum of $\tilde{\phi}$; (b) power spectrum of $\tilde{n}_e/n_e$; (c),(d) coherence and phase between $\tilde{\phi}$ and $\tilde{n}_e/n_e$. Measurements are taken at $r/a \sim 0.33$–0.42.

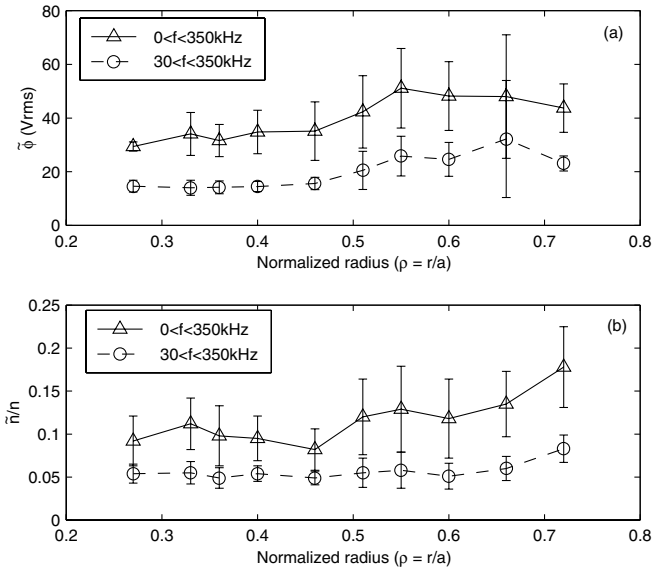

FIG. 4. Radial profiles of (a) $\tilde{\phi}(r)$ and (b) $\tilde{n}_e(r)/n_e$ for the standard $I_p \sim 380$ kA plasmas in MST.

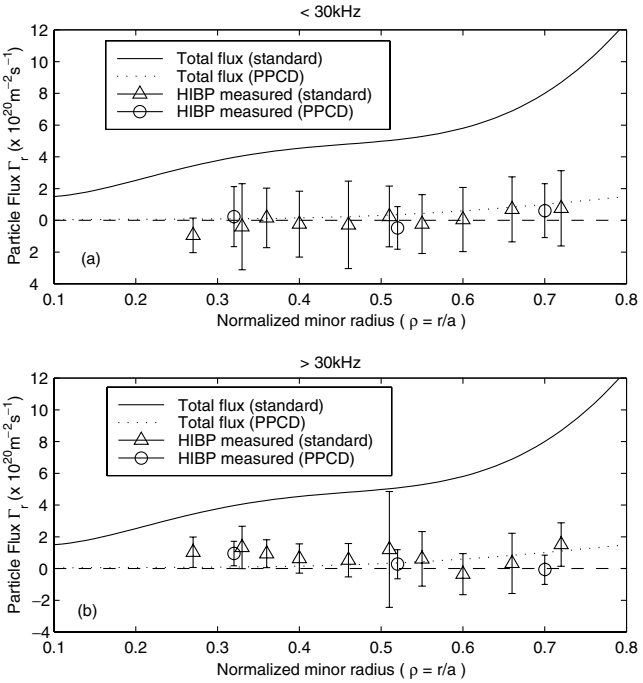

FIG. 5. Measured fluctuation induced particle transport profiles: (a) <30 kHz and (b) > 30 kHz. △ for the standard 380 kA plasmas and ∘ for the 390 kA PPCD plasmas. Solid and dotted lines are the total flux densities for the standard and PPCD discharges, respectively. Error bars indicate standard deviations.

measurement range of $r/a = 0.25$–0.7. It is also found that the shapes of the standard and PPCD profiles of the MHD correlated part of $\tilde{n}_e/n_e$ are similar to the results from previous FIR measurements [12].

The electrostatic fluctuation induced radial electron transport is given by

$$\Gamma_r^E = \frac{(\bar{k}_\phi B_\theta - \bar{k}_\theta B_\phi)[P_n P_\phi]^{1/2} \gamma_{n\phi} \sin\theta_{n\phi}}{|B|^2}, \qquad (1)$$

where k_ϕ and k_θ are wave numbers in toroidal and poloidal directions, P_n and P_ϕ are the power spectra densities of $\tilde{n}_e/n_e$ and $\tilde{\phi}$, $\gamma_{n\phi}$ and $\theta_{n\phi}$ are, respectively, the coherence and phase between $\tilde{n}_e/n_e$ and $\tilde{\phi}$. Integration of the expression above and evaluation utilizing HIBP measured quantities results in an estimate of the total electrostatic particle transport due to fluctuations. The present HIBP setup is unable to resolve k_θ and k_ϕ as is typically done from its two point measurements [13]. Thus, we use the alternative method of estimating their values by dividing the spectrum into <30 kHz and > 30 kHz regions. For $f < 30$ kHz, $m/n = 1/6$ mode dominates and thus $k_\phi \sim k_\theta \sim m/r \sim n/R \sim 4$ m^{-1}. For $f > 30$ kHz, assuming the perturbations are propagating at about the same velocity as the measured plasma flow velocity, which is ~30 km/s, then the wave numbers estimated in this manner range from 6–40 m^{-1} (up to 200 kHz), which are comparable to previous edge Langmuir probe results [14]. Above 200 kHz, no coherence is found between $\tilde{n}$ and $\tilde{\phi}$. Utilizing these wave numbers and the measured $\tilde{n}_e$ and $\tilde{\phi}$, the electrostatic induced electron fluxes are estimated and plotted in Figs. 5(a) and 5(b) for low frequency (< 30 kHz) and high frequency (> 30 kHz), respectively. For comparative purposes, the total fluxes, predicted by particle balance through the measurement of the density profile and particle source, are shown for each case.

Within the measurement uncertainties, the electrostatic fluctuation induced particle transport estimated by the HIBP measurements is too small to account for the total particle flux in a standard plasma. These results are consistent with the RFP transport model: within the reversal surface, the magnetic fluctuations dominate the particle flux and the electrostatic transport is small in the core of MST. This is the first experimental verification that electrostatic transport is small in the core of standard RFP plasmas. While the total particle transport is greatly reduced in a PPCD discharge, the estimated electrostatic fluxes remain small, bracketing the total particle transport within the error bars.

In summary, we have successfully demonstrated the ability of the MST-HIBP to simultaneously measure plasma potential fluctuations $\tilde{\phi}$ and relative electron-density fluctuations $\tilde{n}_e/n_e$ in the core of a hot RFP plasma. These first experimental measurements of concurrent electrostatic fluctuations have enabled us to confirm that electrostatic particle transport is too small to account for the total particle flux. The successful application of a beam probe on MST is predicated on the development of novel crossover sweep systems and magnetic plasma suppression structures. Although substantial

equilibrium changes during sawtooth periods limit measurements to duration of the discharge between sawtooth events, some improvements in hardware, such as the addition of a feedback control, may extend measurements to a full sawtooth period, thus enabling the study of additional important physics issues, such as discrete dynamo events and magnetic reconnections.

We are grateful for many useful discussions with Professor S. Prager, Professor C. Forest, Dr. J. Sarff, Dr. D. Craig, and the help from the members of the MST group. This work is supported by the U.S. Department of Energy.

[1] J. B. Taylor, Phys. Rev. Lett. **33**, 1139 (1974).
[2] H. A. B. Bodin and A. A. Newton, Nucl. Fusion **20**, 1255 (1980).
[3] P. C. Liewer, Nucl. Fusion **25**, 543 (1985).
[4] T. D. Rempel *et al.*, Phys. Rev. Lett. **67**, 1438 (1991).
[5] G. A. Hallock, A. J. Wootton, and R. L. Hickok, Phys. Rev. Lett. **59**, 1301 (1987).
[6] K. Saadatmand, T. P. Crowley, and R. L. Hickok, Jr., Phys. Fluids B **1**, 164 (1989).
[7] S. C. Aceto, K. A. Connor, J. G. Schwelberger, and J. J. Zielinski, IEEE Trans. Plasma Sci. **22**, 388 (1994).
[8] J. C. Forster, P. M. Schoch, R. L. Hickok, and W. C. Jennings, IEEE Trans. Plasma Sci. **22**, 359 (1994).
[9] D. R. Demers *et al.*, Phys. Plasmas **8**, 1278 (2001).
[10] J. Lei *et al.*, Rev. Sci. Instrum. **70**, 967 (1999).
[11] J. Lei, Ph.D. dissertation, Rensselaer Polytechnic Institute, 2002.
[12] N. E. Lanier *et al.*, Phys. Plasmas **8**, 3402 (2001).
[13] T. P. Crowley, IEEE Trans. Plasma Sci. **22**, 291 (1994).
[14] C. S. Chiang, Ph.D. thesis, University of Wisconsin–Madison, 2000.